1
2
3
4
5
6
7
8
9
10
11
12
13
14
15
16
17
18
19
20
21
22
23
24
25
26
27
28
29
30
31
32
33
34
35
36
37
38
39
40
41
42
43
44
45
46
47
48
49
50
51
52
53
54
55
56
57
58
59
60

The Prototypical Transition Metal Carbenes, $(CO)_5Cr=CH_2$, $(CO)_4Fe=CH_2$, $(CO)_3Ni=CH_2$, $(CO)_5Mo=CH_2$, $(CO)_4Ru=CH_2$, $(CO)_3Pd=CH_2$, $(CO)_5W=CH_2$, $(CO)_4Os=CH_2$, and $(CO)_3Pt=CH_2$: Challenge to Experiment

Jared D. Weidman, Marissa L. Estep, and Henry F. Schaefer III*

Center for Computational Quantum Chemistry, University of Georgia, Athens, GA 30602, USA

E-mail: ccq@uga.edu

July 26, 2018

Abstract

Transition metal carbenes are useful in organometallic chemistry due to their demonstrated use as catalysts in carbon-carbon bond forming reactions. Yet, the prototypical transition metal carbenes—consisting of a single metal center doubly bonded to a methylene ligand and surrounded by carbonyls—have been elusive to experimental synthesis. This theoretical work examines the structures and properties of nine prototypical transition metal carbenes. Optimized values for $M=CH_2$ bond lengths, dissociation energies, and vibrational frequencies are reported. The $M=CH_2$ bond distances range from 1.81 Å (Ni) to 2.05 Å (Pd). The $M=CH_2$ dissociation energies fall in the range of 16.4 kcal mol^{-1} (Pd) to 92.3 kcal mol^{-1} (Os). The spectroscopic observation of several of these molecules should be possible.

Introduction

Transition metal carbenes have gained considerable interest in the organometallic chemistry community due to their usefulness in the synthesis of many organic compounds. These complexes have had widespread use as catalysts in olefin metathesis processes,[1] and they have been used in alkene cyclopropanation and carbonyl alkenation reactions.[2] Transition metal carbenes are generally categorized as Fischer carbenes[3] or Schrock carbenes[4] based on their bonding characteristics.

The bonding in Fischer-type transition metal carbenes is often understood in terms of the Dewar-Chatt-Duncanson (DCD) model (Figure 1a).[5] In this model, the double bond between the metal and ligand can be considered the result of σ donation from the carbon to the metal and π back-donation from the metal to the carbon. The bonding in Schrock carbenes, meanwhile, can be understood as a traditional double bond where both the metal and carbon share two σ and two π electrons (Figure 1b). Schrock carbenes are more accurately described as alkylidenes due to this bonding character.

Figure 1: Schematic of the typical bonding patterns in (a) Fischer carbenes and (b) Schrock carbenes.
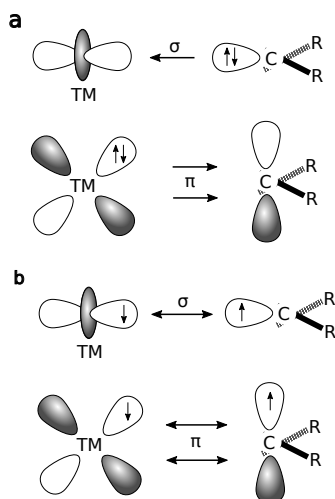
This work considers prototypical transition metal carbenes—the simplest possible transition metal carbenes, in the expectation that they should be experimentally viable. With

these guidelines in mind, the simplest realistic transition metal carbenes would consist of the simplest carbene ligand, methylene, attached to a single metal center in a neutral complex that obeys the eighteen electron rule.[6,7] These prototypical carbenes would be of the form $(CO)_5M=CH_2$, $(CO)_4M=CH_2$, or $(CO)_3M=CH_2$, where M is a metal from group 6, 8, or 10, respectively. Transition metal carbonyl complexes are well-known both theoretically and experimentally,[8–11] making carbonyl ligands a logical choice to occupy the rest of the coordination sphere. The molecules that were initially studied in this research include $(CO)_5Cr=CH_2$, $(CO)_4Fe=CH_2$, and $(CO)_3Ni=CH_2$. We further consider second and third-row transition metals of groups 6, 8, and 10, namely $(CO)_5Mo=CH_2$, $(CO)_5W=CH_2$, $(CO)_4Ru=CH_2$, $(CO)_4Os=CH_2$, $(CO)_3Pd=CH_2$, and $(CO)_3Pt=CH_2$.

None of the transition metal carbenes investigated in this study has been synthesized experimentally. This is likely due to the high reactivity of the carbene carbon; the two hydrogens offer minimal steric hindrance to approach of potential coreactants.[6] Transition metal carbenes have been synthesized with larger R groups on the carbon.[12,13] Further, many molecules have been reported with $M=CH_2$ bonds. These are generally Schrock-type transition metal carbenes with ligands other than carbonyls surrounding the metal center. Schrock in 1975 isolated and characterized the first transition-metal methylene complex, $Ta(\eta^5-C_5H_5)_2-(CH_3)(CH_2)$.[4] In 2015, Chen and coworkers proposed a complex with a $Ni=CH_2$ double bond as an intermediate in a nickel-catalyzed cyclopropanation scheme.[14] A 2017 study by Levine, Tilley, and Anderson found evidence for short-lived $Y=CH_2$ and $Sc=CH_2$ bonds.[15] The first structurally characterized alkilydenes of hexavalent chromium have recently been reported.[16]

The experimental study most closely related to this research is the photoionization mass spectrometry work of Beauchamp and coworkers on gas-phase $(CO)_5Mn^+=CH_2$,[17,18] isoelectronic to $(CO)_5Cr=CH_2$. A very substantial dissociation energy of 104 ± 3 kcal mol^{-1} was reported for this species. It should also be noted that the "naked" cationic M^+-CH_2 complexes of Cr, Fe, and Ni have been made in the gas phase, and experimental values for the

bond energies have been reported to be 65 ± 7 kcal mol^{-1}, 96 ± 5 kcal mol^{-1}, and 86 ± 6 kcal mol^{-1}, respectively.[19]

The first theoretical study on one of these prototypical transition metal carbenes was in 1981 when Spangler et al. studied $(CO)_3Ni=CH_2$ at the SCF level of theory.[6] Optimized geometrical parameters for this molecule were compared to those obtained for the naked $Ni=CH_2$ and the homoleptic carbonyl $Ni(CO)_4$. The minimum energy structure was found to be of C_s symmetry with the CH_2 staggered with respect to all the carbonyls. In 1984, Taylor and Hall[20] used a generalized molecular orbital (GMO) approach to study a number of simple carbene systems, including $(CO)_5Mo=CH_2$. A dissociation energy of 56 kcal mol^{-1} was computed for this complex. The C_{2v} staggered conformation was found to be the lowest energy structure. In 1992, Márquez and Fernández Sanz[21] studied the $(CO)_5Mo=CH_2$ complex using the complete active space self-consistent field (CASSCF) method. The system was not found to be significantly multireference, with a leading CAS coefficient (unsquared) of 0.94. In addition to optimized geometries and dissociation energies, Márquez and Fernández Sanz reported potential energy profiles for dissociation.

The most relevant theoretical studies on these transition metal carbene systems were done by the groups of Ziegler and Frenking starting in the mid-1990s. Ziegler and coworkers[22] studied the three group 6 metal complexes (Cr, Mo, W) using the local density approximation (LDA) and a triple-ζ Slater-type orbital (STO) basis set. They reported the effects of including nonlocal density corrections and relativistic effects on the bond lengths and energies. The chromium complex was also included as part of their 1995 study that examined a number of different chromium carbenes and silylenes.[23] The $Cr=CH_2$ bond was found to be the shortest of all the $Cr–CR_2$ and $Cr–SiR_2$ bonds studied, namely 1.88 Å. A later 1996 study by the Ziegler group found that this relatively short bond length is due to a strong energetic match between the metal 3d donor orbital and the acceptor orbital on the methylene carbon.[24]

In 1996, Frenking and coworkers[25] reported an *ab initio* study on the three group 6 (Cr,

Mo, W) and three group 10 (Ni, Pd, Pt) transition metal carbene complexes. Optimized geometries were obtained at the MP2/6-31G(p) level of theory, and energies were obtained at the CCSD(T) level. In addition, charge decomposition analysis (CDA) was done to estimate the amount of donation and back-donation occurring from the ligand to the metal and vice versa. The CH_2 ligand was found to be both a strong electron donor and a strong electron acceptor. Vyboishchikov and Frenking (1998) analyzed the bonding of Fischer-type (e.g. $(CO)_5W=CR_2$) and Schrock-Type (e.g. $F_4W=CR_2$) complexes of tungsten using the CDA method in addition to Bader's atoms in molecules (AIM) theory and the natural bond orbital (NBO) partitioning scheme.[26] They found that the metal–carbon bonding in the complex $(CO)_5W=CH_2$ can be interpreted as a Fischer-type donor-acceptor relationship as opposed to a traditional double bond.

In 2000, Frenking and coworkers studied $(CO)_4Fe=CH_2$ using the B3LYP/6-31G(d) method for geometry optimizations and CCSD(T) for energies.[27] The C_{2v} eclipsed structure with equatorial CH_2 was found to lie lower in energy than the C_s axial structure by around 8 kcal mol^{-1}. The $(CO)_4Fe=CH_2$ system was also studied in 2001 by Frenking and coworkers as part of a larger study on iron carbenes with various ligands.[28] Frenking and coworkers in 2002 revisited $(CO)_5Cr=CH_2$ as part of a larger study on the effects of changing the ligand on transition metal carbene complexes.[29] This study was done using the BP86 functional and a triple-ζ STO basis set. Frenking also published two helpful reviews in the 2000s on the bonding in transition-metal carbene complexes.[5,30] Several other theoretical studies exist that mention one or more of the complexes studied here.[31–34]

The classification of these prototypical transition metal carbenes as Fischer or Schrock carbenes is a bit ambiguous. Methylene is well-known to have a triplet ground state,[35] which taken on its own suggests that a Schrock-type double bond forms in these complexes between a triplet metal carbonyl fragment and a triplet methylene ligand. However, the metal centers studied here are middle to late transition metals with low oxidation states (0), which are more characteristic of the singlet-singlet donation/back-donation bonding of

Fischer carbenes. Indeed, the literature generally classifies the carbenes considered here as Fischer carbenes.[22,26]

To date, no theoretical study exists that examines all nine transition metal carbenes considered here. The $(CO)_4Ru=CH_2$ and $(CO)_4Os=CH_2$ complexes in particular have never been studied theoretically. More importantly, none of these complexes has ever been made or studied experimentally. In addition to optimized geometries, $M=CH_2$ bond properties such as dissociation energies and vibrational frequencies will be predicted here. There is a lack of vibrational frequencies reported in the literature on these complexes, as none of the previous theoretical studies mentioned here report all of these values. Trends in these properties as the metal center is changed will be examined in terms of both top-to-bottom and left-to-right movement on the periodic table. We hope our results on the chemistry of these complexes will motivate experimental investigations.

The primary theoretical method that will be used in this research is density functional theory (DFT). There has been considerable development in DFT methods in the 15 years since the last theoretical studies on transition metal carbenes.[36] In particular, the M06-L, ωB97X, and related functionals have experienced considerable use and have been shown to perform well in numerous applications, including transition metal complexes.[37]

Theoretical Methods

For this study, we used five different DFT functionals, all of which are well-known and have been used extensively on transition metal systems: B3LYP, BP86, M06-L, ωB97X, and ωB97X-D3. B3LYP is a hybrid generalized gradient approximation (GGA) functional consisting of Becke's three-parameter exchange and the correlation functional of Lee, Yang, and Parr.[38,39] BP86 is a GGA functional consisting of Becke's 1988 exchange functional and Perdew's 1986 correlation functional.[38,40] M06-L, a meta-GGA functional, is from the Minnesota family of functionals and was designed to model transition metal bonding.[41]

The ωB97X functional is a hybrid-meta GGA functional.[42] The last functional is ωB97X-D3, which is a re-optimization of ωB97X-D with an improved dispersion correction from Grimme.[43] ωB97X-D, a version of ωB97X with dispersion effects included, has been shown to perform the best out of 25 functionals studied for geometry optimizations of transition metal complexes.[37] The ωB97X-D3 functional should be a further improvement over those results. The transition metal carbenes studied in this research are not expected to have significant long-range interactions. By comparing the results of ωB97X versus ωB97X-D3, any dispersion effects present can be monitored.

The cc-pVTZ basis set was used for all atoms except the second and third row transition metals, for which a cc-pVTZ-PP basis set was employed.[44] DFT is generally not as sensitive to basis set size as are wavefunction-based methods,[45] so cc-pVTZ should be sufficiently large to obtain reliable results. The use of the cc-pVTZ-PP basis set on the second and third row transition metals is due to the need for effective core potentials (ECPs) for these atoms. The use of ECPs allows for significant speedup in addition to the inclusion of relativistic effects. The relativistic ECPs of the Stuttgart group[46,47] were used in this work.

These computations were performed using the ORCA 4.0 software package.[48] The finest DFT grid setting was used, consisting of a Lebedev 770 point grid, to minimize integration grid errors.[49] For hybrid functionals, the RIJCOSX approximation[50,51] was used to speed up the computation of the Hartree-Fock exchange term.

Results and Discussion

The following sections explore the optimized geometries, metal-carbene dissociation energies, and metal-carbene stretching frequencies obtained for the nine complexes considered here. All carbene complexes were determined to have singlet ground states. These singlet states generally were found to be at least 20 kcal mol^{-1} lower in energy than the analogous triplet states. The complex with the closest singlet-triplet splitting was $(CO)_3Pd=CH_2$ for which

this gap was found to be 2 kcal mol^{-1}. A complete collection of optimized Cartesian coordinates, vibrational frequencies, and energies for all singlet and triplet complexes considered here is given in the Supporting Information.

Optimized Geometries

Figure 2:   Optimized geometries (B3LYP/cc-pVTZ) of $(CO)_5M=CH_2$ (M = Cr, Mo, W) complexes. Relevant geometrical parameters are given in Table 1

$(CO)_5Cr=CH_2$

$(CO)_5Mo=CH_2$

$(CO)_5W=CH_2$
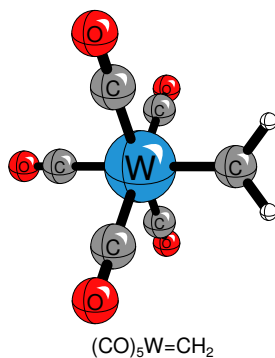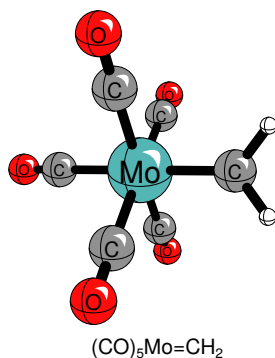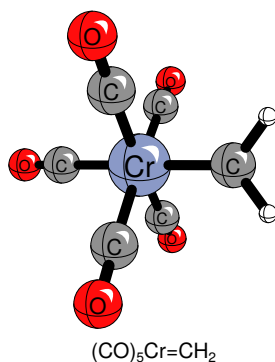
Optimized structures for the nine transition metal carbene complexes are shown in Fig-

Figure 3: Optimized geometries (B3LYP/cc-pVTZ) of $(CO)_4M=CH_2$ (M = Fe, Ru, Os) complexes. Relevant geometrical parameters are given in Table 2

$(CO)_4Fe=CH_2$

$(CO)_4Ru=CH_2$

$(CO)_4Os=CH_2$

1
2
3
4
5
6
7
8
9
10
11
12
13
14
15
16
17
18
19
20
21
22
23
24
25
26
27
28
29
30
31
32
33
34
35
36
37
38
39
40
41
42
43
44
45
46
47
48
49
50
51
52
53
54
55
56
57
58
59
60
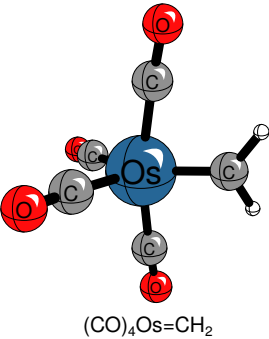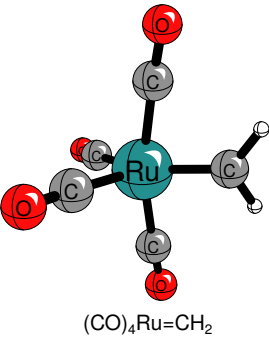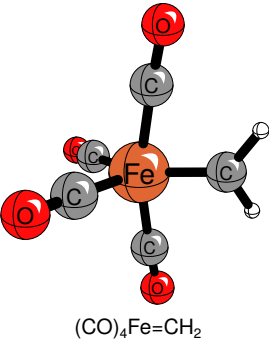
Figure 4: Optimized geometries (B3LYP/cc-pVTZ) of $(CO)_3M=CH_2$ (M = Ni, Pd, Pt) complexes. Relevant geometrical parameters are given in Table 3

$(CO)_3Ni=CH_2$

$(CO)_3Pd=CH_2$

$(CO)_3Pt=CH_2$
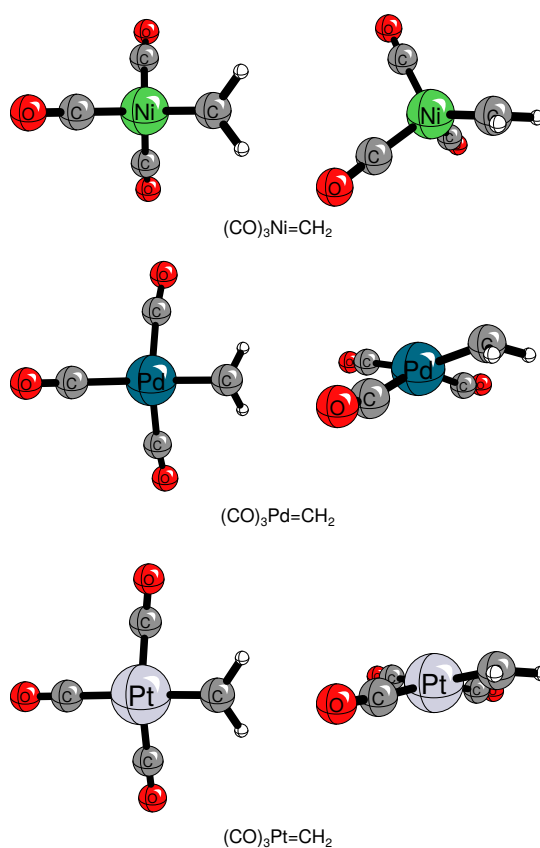
Table 1: Optimized bond distances (angstroms) and methylene rotation dihedral angles (degrees) in $(CO)_5M=CH_2$ (M = Cr, Mo, W) complexes from five DFT functionals. Structures are shown in Figure 2. The subscript "cis" refers to the four equivalent carbonyls, while "trans" refers to the one carbonyl opposite the methylene.

	B3LYP	BP86	M06-L	ωB97X	ωB97X-D3
$Cr–C_m$	1.91	1.92	1.91	1.89	1.89
$Cr–C_{cis}$	1.93	1.91	1.92	1.92	1.91
$Cr–C_{trans}$	1.96	1.94	1.96	1.96	1.95
$C_m–H$	1.09	1.10	1.09	1.10	1.09
$C_{cis}–O$	1.14	1.15	1.14	1.14	1.14
$C_{trans}–O$	1.14	1.15	1.14	1.13	1.13
$\angle(H\text{-}C_m\text{-}Cr\text{-}C_{cis})$	44.1	43.5	43.5	44.1	44.0
$Mo–C_m$	2.04	2.05	2.04	2.01	2.02
$Mo–C_{cis}$	2.08	2.07	2.08	2.08	2.07
$Mo–C_{trans}$	2.13	2.11	2.14	2.14	2.13
$C–H$	1.09	1.10	1.10	1.09	1.09
$C_{cis}–O$	1.14	1.15	1.14	1.14	1.14
$C_{trans}–O$	1.14	1.15	1.14	1.13	1.13
$\angle(H\text{-}C_m\text{-}Mo\text{-}C_{cis})$	43.9	43.2	42.9	43.8	43.8
$W–C_m$	2.05	2.06	2.05	2.03	2.03
$W–C_{cis}$	2.08	2.07	2.08	2.07	2.07
$W–C_{trans}$	2.12	2.11	2.12	2.12	2.11
$C–H$	1.09	1.10	1.09	1.09	1.09
$C_{cis}–O$	1.14	1.16	1.15	1.14	1.14
$C_{trans}–O$	1.14	1.15	1.14	1.14	1.14
$\angle(H\text{-}C_m\text{-}W\text{-}C_{cis})$	43.7	43.1	42.8	43.6	43.7

1
2
3
4
5
6
7
8
9
10
11
12
13
14
15
16
17
18
19
20
21
22
23
24
25
26
27
28
29
30
31
32
33
34
35
36
37
38
39
40
41
42
43
44
45
46
47
48
49
50
51
52
53
54
55
56
57
58
59
60

Table 2: Optimized bond distances (angstroms) in $(CO)_4M=CH_2$ (M = Fe, Ru, Os) complexes from five DFT functionals. Structures are shown in Figure 3. The subscript "cis" refers to the two equivalent axial carbonyls bent toward the methylene, while "trans" refers to the two carbonyls oriented away from the methylene.

	B3LYP	BP86	M06-L	ωB97X	ωB97X-D3
Fe–C_m	1.84	1.85	1.84	1.82	1.82
Fe–C_{cis}	1.82	1.80	1.82	1.81	1.81
Fe–C_{trans}	1.82	1.81	1.82	1.82	1.81
C_m–H	1.09	1.10	1.09	1.09	1.09
C_{cis}–O	1.14	1.15	1.14	1.13	1.13
C_{trans}–O	1.14	1.15	1.14	1.13	1.13
Ru–C_m	1.95	1.96	1.95	1.93	1.93
Ru–C_{cis}	1.96	1.95	1.96	1.96	1.95
Ru–C_{trans}	1.96	1.95	1.96	1.96	1.95
C_m–H	1.09	1.10	1.09	1.09	1.09
C_{cis}–O	1.14	1.15	1.14	1.13	1.13
C_{trans}–O	1.14	1.15	1.14	1.14	1.14
Os–C_m	1.97	1.97	1.97	1.95	1.95
Os–C_{cis}	1.97	1.96	1.96	1.96	1.96
Os–C_{trans}	1.96	1.95	1.95	1.95	1.95
C_m–H	1.09	1.09	1.09	1.09	1.09
C_{cis}–O	1.14	1.15	1.14	1.13	1.13
C_{trans}–O	1.14	1.16	1.15	1.14	1.14

Table 3: Optimized bond distances (angstroms) and angles (degrees) in $(CO)_3M=CH_2$ (M = Ni, Pd, Pt) complexes from five DFT functionals. Structures are shown in Figure 4. The subscript "trans" refers to the carbonyl lying in the reflection plane of symmetry, while "cis" refers to the two equivalent carbonyls lying outside the reflection plane.

	B3LYP	BP86	M06-L	ωB97X	ωB97X-D3
Ni–C_m	1.83	1.83	1.83	1.81	1.81
Ni–C_{trans}	1.82	1.81	1.82	1.82	1.81
Ni–C_{cis}	1.86	1.83	1.85	1.86	1.85
C_m–H	1.09	1.10	1.10	1.10	1.10
C_{trans}–O	1.14	1.15	1.14	1.13	1.13
C_{cis}–O	1.14	1.15	1.14	1.13	1.13
$\angle(C_m\text{-}Ni\text{-}C_{trans})$	123.4	122.8	123.4	121.2	121.7
$\angle(H\text{-}C_m\text{-}Ni\text{-}C_{cis})$	23.7	22.6	21.9	26.3	25.7
Pd–C_m	2.07	2.05	2.07	2.05	2.05
Pd–C_{trans}	2.16	2.10	2.17	2.19	2.17
Pd–C_{cis}	2.12	2.06	2.12	2.17	2.14
C_m–H	1.10	1.10	1.10	1.10	1.10
C_{trans}–O	1.13	1.15	1.14	1.13	1.13
C_{cis}–O	1.13	1.15	1.14	1.13	1.13
$\angle(C_m\text{-}Pd\text{-}C_{trans})$	158.0	158.8	160.3	153.8	153.7
$\angle(H\text{-}C_m\text{-}Pd\text{-}C_{cis})$	-7.9	-8.8	-11.3	-1.8	-2.1
Pt–C_m	1.96	1.96	1.97	1.93	1.94
Pt–C_{trans}	1.97	1.95	1.96	1.96	1.96
Pt–C_{cis}	1.93	1.92	1.93	1.93	1.93
C_m–H	1.08	1.09	1.09	1.09	1.09
C_{trans}–O	1.14	1.15	1.14	1.13	1.13
C_{cis}–O	1.14	1.15	1.14	1.13	1.13
$\angle(C_m\text{-}Pt\text{-}C_{trans})$	166.4	165.8	166.5	165.7	165.7
$\angle(H\text{-}C_m\text{-}Pt\text{-}C_{cis})$	-1.2	-0.3	-2.4	-0.7	-0.5

ures 2, 3, 4 for the complexes of metals in groups 6, 8, or 10, respectively. The figures shown were generated from B3LYP coordinates, but all five functionals gave the same general structures. The most relevant bond and angle parameters for the group 6, group 8, and group 10 complexes are given in Tables 1, 2, and 3, respectively.

The group 6 complexes of Cr, Mo, and W were found to exhibit C_{2v} minima where the methylene group is staggered with respect to the carbonyls. We distinguish between the carbonyl carbons by referring to the four equivalent carbonyl carbons as C_{cis} and the carbon in the rotational axis across from the methylene group as C_{trans}. There is little variation in the general structure between the complexes of the group 6 metals. The octahedral coordination remains largely unchanged moving to the metals lower on the periodic table. The largest difference between the complexes is in the bond distances. The M–C distances for the compounds of Mo and W are around 0.1-0.2 Å longer than the corresponding bonds from the Cr complex.

The group 8 complexes also have C_{2v} minimum energy structures. These complexes exhibit trigonal-bipyramidal-type structures, where the two axial carbonyls are slightly bent towards the methylene. The methylene group prefers the equatorial position where the hydrogens are rotated to be eclipsed with respect to the two nearest carbonyls. We label these two axial carbonyls as C_{cis} and the two equatorial carbonyls as C_{trans}. Similarly to the group 6 complexes, the structures are relatively unchanged as the metal center is changed. The main difference between the complexes is that the complexes of Ru and Os both have M–C bond distances that are about 0.10 to 0.15 Å longer than the Fe complex.

The group 10 minimum energy structures are of C_s symmetry. The methylene group in the Ni complex is rotated to be staggered with respect to all the carbonyls. We label the carbonyl carbon that lies in the plane of reflection as C_{trans}, and the carbons out of the plane of symmetry are labeled C_{cis}. In contrast to the group 6 and group 8 complexes, the group 10 complexes exhibit significant structural changes as the metal center is changed. While the Ni complex has a roughly tetrahedral-type structure, the Pd and Pt complexes

are significantly flatter, with the Pt complex being nearly planar. The methylene in these flatter complexes is rotated to be essentially eclipsed with respect to the cis carbonyls.

A referee has noted the existence of another conformer of the Pd complex with a shorter M–C_m bond and one long M–CO bond. We have found this conformer with four of the five DFT functionals (B3LYP, M06-L, ωB97X, ωB97X-D3). The Pd–C_{trans} bond in this conformer was found to range from 2.9-3.3 Å, and the relative electronic energy compared to the standard Pd conformer ranges from –1.8 to +0.5 kcal mol^{-1}. Complete details on this other conformer are given in the Supporting Information.

The five functionals are in general agreement on the geometrical parameters in Tables 1, 2, and 3. For a given complex, the M=C distances never differ by more than a few hundredths of an angstrom between functionals. The inclusion of dispersion for the ωB97X-D3 functional does not appear to make a large difference; the bond distances from ωB97X and ωB97X-D3 are never more than 0.01 Å different. This result makes sense, as these complexes are not expected to exhibit significant long-range effects that would influence their bonding.

The metal–methylene bond distances for all nine complexes are compared in Table 4. The ωB97X and ωB97X-D3 functionals tend to be shorter than those obtained by the other functionals by around 0.02 Å, while the other three agree with each other. In general, the M=CH_2 bond distances increase going down a given group in the periodic table and decrease going to the right across a row. The big exception to these trends is the $(CO)_3Pd=CH_2$ complex, for which the longest M=CH_2 distance of 2.07 Å was found with B3LYP and M06-L.

Dissociation Energies

Dissociation energies for the M=CH_2 bond in the nine transition metal carbenes are reported in Figure 5 and Table 5. These dissociation energies were computed using the ground state energies of each of the fragments involved. The transition metal carbenes and the transition metal carbonyl fragments were computed as singlets, while methylene was computed as a

Figure 5: M=CH$_2$ dissociation energies (kcal mol^{-1}) in transition metal carbene complexes from five DFT functionals.
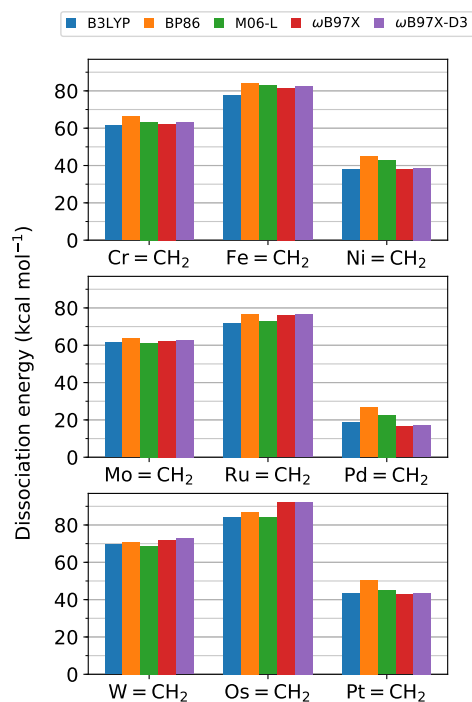
Table 4: $M=CH_2$ bond lengths (Å) in transition metal carbene complexes from five DFT functionals.

	$Cr=CH_2$	$Fe=CH_2$	$Ni=CH_2$
B3LYP	1.91	1.84	1.83
BP86	1.92	1.85	1.83
M06-L	1.91	1.84	1.83
ωB97X	1.89	1.82	1.81
ωB97X-D3	1.89	1.82	1.81
	$Mo=CH_2$	$Ru=CH_2$	$Pd=CH_2$
B3LYP	2.04	1.95	2.07
BP86	2.05	1.96	2.05
M06-L	2.04	1.95	2.07
ωB97X	2.01	1.93	2.05
ωB97X-D3	2.02	1.93	2.05
	$W=CH_2$	$Os=CH_2$	$Pt=CH_2$
B3LYP	2.05	1.97	1.96
BP86	2.06	1.97	1.96
M06-L	2.05	1.97	1.97
ωB97X	2.03	1.95	1.93
ωB97X-D3	2.03	1.95	1.94

triplet. This method of computing dissociation energies agrees with the methods used by Taylor and Hall[20] and by Frenking,[25] but is different from the methods used by Márquez and Fernández Sanz[21] and by Ziegler,[22] who take into account conservation of spin for the dissociating fragments. Such methods compute the dissociation energy using the lowest singlet state of methylene, which lies around 9 kcal mol^{-1} higher in energy than the ground state triplet. Dissociation energies from these spin-conserving methods will be inherently shifted around 9 kcal mol^{-1} higher than the dissociation energies reported here.

There is more variation between functionals for the computation of dissociation energies than for the geometrical parameters. While the five functionals give the same general trends and conclusions, the dissociation energies for a given system can vary by over 10 kcal mol^{-1} depending on the functional used. These discrepancies are most significant for the weakly bound $(CO)_3Pd=CH_2$ complex, the difference between the dissociation computed from ωB97X (16.4 kcal mol^{-1}) and BP86 (26.7 kcal mol^{-1}) is 10.3 kcal mol^{-1}, a significant variation for an energy on the order of 20 kcal mol^{-1}. The BP86 functional overall tends to

Table 5:　M=CH$_2$ dissociation energies (kcal mol^{-1}) in transition metal carbene complexes from five DFT functionals.

	Cr=CH$_2$	Fe=CH$_2$	Ni=CH$_2$
B3LYP	61.3	77.6	37.8
BP86	66.4	83.8	45.0
M06-L	63.3	83.0	42.7
wB97X	62.3	81.5	37.8
wB97X-D3	63.2	82.5	38.7
	Mo=CH$_2$	Ru=CH$_2$	Pd=CH$_2$
B3LYP	61.4	71.9	18.9
BP86	63.5	76.8	26.7
M06-L	61.1	72.8	22.7
wB97X	62.4	75.9	16.4
wB97X-D3	62.9	76.6	17.0
	W=CH$_2$	Os=CH$_2$	Pt=CH$_2$
B3LYP	69.6	84.3	43.4
BP86	71.0	86.8	50.4
M06-L	68.7	84.0	44.8
wB97X	72.1	92.3	42.7
wB97X-D3	72.7	92.3	43.7

produce the highest dissociation energies, while B3LYP tends to be the lowest. The ωB97X and ωB97X-D3 functionals produce nearly the same energies. The dispersion effects included in ωB97X-D3 lead to slightly larger dissociation energies than ωB97X, but by no more than 1 kcal mol^{-1}.

The dissociation energies follow the trend of group 8 > group 6 > group 10 for a given row on the periodic table. In addition, the general trend of row 3 > row 1 > row 2 is followed. The (CO)$_3$Pd=CH$_2$ complex once again is an outlier here with a dissociation energy of around 20 kcal mol^{-1}, which is by far the lowest of all complexes reported here. This low dissociation energy combined with the relatively long M=CH$_2$ bond length suggest that this complex is the least likely to be synthesized in the near future. The (CO)$_4$Os=CH$_2$ complex has the overall highest dissociation energies computed with a value of up to 92.3 kcal mol^{-1} from ωB97X-D3.

Vibrational Frequencies

The $M{=}CH_2$ stretching frequencies are reported in Table 6. A complete list of all vibrational frequencies computed is given in the Supporting Information. Two vibrational modes for the $(CO)_5Cr{=}CH_2$ and $(CO)_5Mo{=}CH_2$ complexes correspond to $M{=}CH_2$ stretching, and both are reported. In both of these complexes, neither of these vibrational modes is a pure $M{=}CH_2$ stretch; rather, this stretching mode is coupled to umbrella-type bending motions of the equatorial carbons. For the rest of the molecules, a single obvious mode corresponds to the $M{=}CH_2$ stretch.

The five functionals qualitatively agree with each other for the $M{=}CH_2$ stretching frequency. While the B3LYP, BP86, and M06-L frequencies are generally within around 10 cm^{-1} of each other, the ωB97X and ωB97X-D3 functionals are generally around 50 cm^{-1} higher.

The frequency results do not exhibit clear periodic trends as did the bond lengths and dissociation energies. The $(CO)_3Pd{=}CH_2$ complex does have the lowest $M{=}CH_2$ stretching frequency in the range of 505-532 cm^{-1}, which is unsurprising given its long $M{=}CH_2$ bond and low dissociation energy. The $(CO)_4Fe{=}CH_2$ complex is expected to have the largest frequency with a range of 710-770 cm^{-1}.

Insight into the bonding in transition metal carbene complexes may be gained also from considering the normal modes involving the carbonyls in these complexes. Tolman's electronic parameter (TEP), determined from the totally symmetric CO stretching mode of $(CO)_3Ni{-}L$ complexes, has been used as an estimator of the electron donating ability of a ligand.[34,52] The CO stretching frequency of the carbonyl in the *trans* position to the carbene ligand has also been used as a monitor of the electronic properties of the ligand. Tabulations of these two CO stretching frequencies can be found in the Supporting Information.

Table 6: M=CH$_2$ stretching vibrational frequencies (cm^{-1}) in transition metal carbene complexes from five different DFT functionals. Values separated by a slash indicate cases where two M=CH$_2$ stretching frequencies were found.

	Cr=CH$_2$	Fe=CH$_2$	Ni=CH$_2$
B3LYP	599/695	718	644
BP86	597/690	710	649
M06-L	598/686	710	629
ωB97X	615/730	770	670
ωB97X-D3	618/732	765	670
	Mo=CH$_2$	Ru=CH$_2$	Pd=CH$_2$
B3LYP	572/623	691	505
BP86	564/615	678	532
M06-L	570/615	685	507
ωB97X	575/651	732	516
ωB97X-D3	578/650	729	520
	W=CH$_2$	Os=CH$_2$	Pt=CH$_2$
B3LYP	622	717	687
BP86	614	703	675
M06-L	610	713	673
ωB97X	661	758	726
ωB97X-D3	659	755	727

Conclusions

This work reports a theoretical study on nine prototypical transition metal carbenes. The five DFT functionals used generally agree for the quantities studied here. The largest discrepancies between functionals are in the dissociation energies, for which discrepancies of up to 10 kcal mol^{-1} were found. The $(CO)_3Pd=CH_2$ complex is an outlier in the group for every quantity studied, with the longest M=CH$_2$ bond length, lowest dissociation energy, and smallest M=CH$_2$ stretching frequency. It is expected to be the most weakly bound of all these compounds. M=CH$_2$ distances were found to increase down a column on the periodic table and decrease from left to right across a row. The dissociation energies, meanwhile, are largest for the group 8 complexes of Fe, Ru, and Os, followed by the group 6 and group 10 complexes. We hope this theoretical characterization of metal-carbene compounds incites interest in their synthesis from the experimental chemistry community.

Acknowledgments

Supporting Information

See the Supporting Information for optimized Cartesian coordinates, vibrational frequencies, and energies for all singlet and triplet species in this study from five DFT functionals. Details on an alternate conformer of the Pd complex as well as tables of CO stretching frequencies are also given in this section.

References

(1) du Toit, J.; van Sittert, C.; Vosloo, H. Metal Carbenes in Homogeneous Alkene Metathesis: Computational Investigations. *J. Organomet. Chem.* **2013**, *738*, 76–91.

(2) Strassner, T. *Metal Carbenes in Organic Synthesis*; Springer Berlin Heidelberg: Berlin, Heidelberg, 2004; Vol. 13; pp 1–20.

(3) Fischer, E. O.; Maasböl, A. On the Existence of a Tungsten Carbonyl Carbene Complex. *Angew. Chem. Int. Edit.* **1964**, *3*, 580–581.

(4) Schrock, R. R. First Isolable Transition Metal Methylene Complex and Analogs. Characterization, Mode of Decomposition, and Some Simple Reactions. *J. Am. Chem. Soc.* **1975**, *97*, 6577–6578.

(5) Frenking, G.; Fröhlich, N. The Nature of the Bonding in Transition-Metal Compounds. *Chem. Rev.* **2000**, *100*, 717–774.

(6) Spangler, D.; Wendoloski, J. J.; Dupuis, M.; Chen, M. M. L.; Schaefer, H. F. Geometry and Electronic Structure of $(CO)_3NiCH_2$. A Model Transition-metal Carbene. *J. Am. Chem. Soc.* **1981**, *103*, 3985–3990.

(7) Davidson, E. R.; Kunze, K. L.; Machado, F. B. C.; Chakravorty, S. J. The Transition Metal-Carbonyl Bond. *Accounts Chem. Res.* **1993**, *26*, 628–635.

(8) Abel, E. W.; Stone, F. G. A. The Chemistry of Transition-Metal Carbonyls: Structural Considerations. *Q. Rev. Chem. Soc.* **1969**, *23*, 325–371.

(9) Abel, E. W.; Stone, F. G. A. The Chemistry of Transition-Metal Carbonyls: Synthesis and Reactivity. *Q. Rev. Chem. Soc.* **1970**, *24*, 498–552.

(10) Werner, H. Complexes of Carbon Monoxide and Its Relatives: An Organometallic Family Celebrates Its Birthday. *Angew. Chem. Int. Edit.* **1990**, *29*, 1077–1089.

(11) Jonas, V.; Thiel, W. Theoretical Study of the Vibrational Spectra of the Transition Metal Carbonyls $M(CO)_6$ [M=Cr, Mo, W], $M(CO)_5$ [M=Fe, Ru, Os], and $M(CO)_4$ [M=Ni, Pd, Pt]. *J. Chem. Phys.* **1995**, *102*, 8474–8484.

(12) Dötz, K. H.; Stendel, J. Fischer Carbene Complexes in Organic Synthesis: Metal-Assisted and Metal-Templated Reactions. *Chem. Rev.* **2009**, *109*, 3227–3274.

(13) Herndon, J. W. The Chemistry of the Carbon-Transition Metal Double and Triple Bond: Annual Survey Covering the Year 2015. *Coordin. Chem. Rev.* **2016**, *329*, 53–162.

(14) Künzi, S. A.; Sarria Toro, J. M.; den Hartog, T.; Chen, P. Nickel-Catalyzed Cyclopropanation with NMe_4OTf and *n*BuLi. *Angew. Chem. Int. Edit.* **2015**, *54*, 10670–10674.

(15) Levine, D. S.; Tilley, T. D.; Andersen, R. A. Evidence for the Existence of Group 3 Terminal Methylidene Complexes. *Organometallics* **2017**, *36*, 80–88.

(16) Wu, P.; Yap, G. P. A.; Theopold, K. H. Structure and Reactivity of Chromium(VI) Alkylidenes. *J. Am. Chem. Soc.* **2018**, *140*, 7088–7091.

(17) Stevens, A. E.; Beauchamp, J. L. Properties and Reactions of Manganese Methylene Complexes in the Gas Phase. The Importance of Strong Metal-Carbene Bonds for Effective Olefin Metathesis Catalysts. *J. Am. Chem. Soc.* **1979**, *101*, 6449–6450.

(18) Stevens, A. E. Ph.D. Thesis, California Institute of Technology, 1981.

(19) Armentrout, P. B.; Halle, L. F.; Beauchamp, J. L. Periodic Trends in Transition Metal-Hydrogen, Metal-Carbon, and Metal-Oxygen Bond Dissociation Energies. Correlation with Reactivity and Electronic Structure. *J. Am. Chem. Soc.* **1981**, *103*, 6501–6502.

(20) Taylor, T. E.; Hall, M. B. Theoretical Comparison Between Nucleophilic and Electrophilic Transition Metal Carbenes Using Generalized Molecular Orbital and Configuration Interaction Methods. *J. Am. Chem. Soc.* **1984**, *106*, 1576–1584.

(21) Márquez, A.; Fernández Sanz, J. Electronic Structure of the Transition-metal-carbene-like Complexes $(CO)_5Mo-M'H_2$ (M′ = Carbon, Silicon, Germanium and Tin). A Theoretical Study Based on Ab Initio CASSCF Calculations. *J. Am. Chem. Soc.* **1992**, *114*, 2903–2909.

(22) Jacobsen, H.; Schreckenbach, G.; Ziegler, T. The Metal Carbon Double Bond in Fischer Carbenes: A Density Functional Study of the Importance of Nonlocal Density Corrections and Relativistic Effects. *J. Phys. Chem.* **1994**, *98*, 11406–11410.

(23) Jacobsen, H.; Ziegler, T. Trends in Structure and Bonding of Fischer Type Chromium Carbenes and Silylenes. A Density Functional Study. *Organometallics* **1995**, *14*, 224–230.

(24) Jacobsen, H.; Ziegler, T. Transition Metal Fischer-Type Complexes. Density Functional

Analysis of the Systems $(CO)_5CrEH_2$ (E = C, Si, Ge, Sn) and $(CO)_5MCH_2$ (M = Mo, W, Mn^+). *Inorg. Chem.* **1996**, *35*, 775–783.

(25) Ehlers, A. W.; Dapprich, S.; Vyboishchikov, S. F.; Frenking, G. Structure and Bonding of the Transition-Metal Carbonyl Complexes $M(CO)_5L$ (M = Cr, Mo, W) and $M(CO)_3L$ (M = Ni, Pd, Pt; L = CO, SiO, CS, N_2, NO^+, CN^-, NC^-, HCCH, CCH_2, CH_2, CF_2, H_2). *Organometallics* **1996**, *15*, 105–117.

(26) Vyboishchikov, S. F.; Frenking, G. Structure and Bonding of Low-Valent (Fischer-Type) and High-Valent (Schrock-Type) Transition Metal Carbene Complexes. *Chem-Eur. J.* **1998**, *4*, 1428–1438.

(27) Chen, Y.; Petz, W.; Frenking, G. Is It Possible to Synthesize a Low-Valent Transition Metal Complex with a Neutral Carbon Atom as Terminal Ligand? A Theoretical Study of $(CO)_4FeC$. *Organometallics* **2000**, *19*, 2698–2706.

(28) Chen, Y.; Hartmann, M.; Frenking, G. Ligand Site Preference in Iron Tetracarbonyl Complexes $Fe(CO)_4L$ (L=CO, CS, N_2, NO^+, CN, NC, η^2-C_2H_4, η^2-C_2H_2, CCH_2, CH_2, CF_2, NH_3, NF_3, PH_3, PF_3, η^2-H_2). *Z. Anorg. Allg. Chem.* **2001**, *627*, 985–998.

(29) Cases, M.; Frenking, G.; Duran, M.; Solà, M. Molecular Structure and Bond Characterization of the Fischer-Type Chromium–Carbene Complexes $(CO)_5CrC(X)R$ (X = H, OH, OCH_3, NH_2, $NHCH_3$ and R = H, CH_3, $CHCH_2$, Ph, C≡CH). *Organometallics* **2002**, *21*, 4182–4191.

(30) Frenking, G.; Solà, M.; Vyboishchikov, S. F. Chemical Bonding in Transition Metal Carbene Complexes. *J. Organomet. Chem.* **2005**, *690*, 6178–6204.

(31) Van Wüllen, C. Molecular Structure and Binding Energies of Monosubstituted Hexacarbonyls of Chromium, Molybdenum, and Tungsten: Relativistic Density Functional Study. *J. Comput. Chem.* **1997**, *18*, 1985–1992.

(32) Poater, J.; Cases, M.; Fradera, X.; Duran, M.; Solà, M. Electron Pairing Analysis of the Fischer-Type Chromium–Carbene Complexes $(CO)_5Cr=C(X)R$ (X=H, OH, OCH$_3$, NH$_2$, NHCH$_3$ and R=H, CH$_3$, CH=CH$_2$, Ph, CCH). *Chem. Phys.* **2003**, *294*, 129–139.

(33) Barcs, B.; Kollár, L.; Kégl, T. Density Functional Study on the Mechanism of Nickel-Mediated Diazo Carbonylation. *Organometallics* **2012**, *31*, 8082–8097.

(34) Kalescky, R.; Kraka, E.; Cremer, D. New Approach to Tolmans Electronic Parameter Based on Local Vibrational Modes. *Inorg. Chem.* **2014**, *53*, 478–495.

(35) Bender, C. F.; Schaefer, H. F. New Theoretical Evidence for the Nonlinearity of the Triplet Ground State of Methylene. *J. Am. Chem. Soc.* **1970**, *92*, 4984–4985.

(36) Cramer, C. J.; Truhlar, D. G. Density Functional Theory for Transition Metals and Transition Metal Chemistry. *Phys. Chem. Chem. Phys.* **2009**, *11*, 10757–10816.

(37) Minenkov, Y.; Singstad, A.; Occhipinti, G.; Jensen, V. R. The Accuracy of DFT-optimized Geometries of Functional Transition Metal Compounds: a Validation Study of Catalysts for Olefin Metathesis and Other Reactions in the Homogeneous Phase. *Dalton T.* **2012**, *41*, 5526–5541.

(38) Becke, A. D. Density-Functional Exchange-Energy Approximation with Correct Asymptotic Behavior. *Phys. Rev. A* **1988**, *38*, 3098–3100.

(39) Lee, C.; Yang, W.; Parr, R. G. Development of the Colle-Salvetti Correlation-energy Formula into a Functional of the Electron Density. *Phys. Rev. B* **1988**, *37*, 785–789.

(40) Perdew, J. P. Density-Functional Approximation for the Correlation Energy of the Inhomogeneous Electron Gas. *Phys. Rev. B* **1986**, *33*, 8822–8824.

(41) Zhao, Y.; Truhlar, D. G. A New Local Density Functional for Main-Group Thermochemistry, Transition Metal Bonding, Thermochemical Kinetics, and Noncovalent Interactions. *J. Chem. Phys.* **2006**, *125*, 194101.

(42) Chai, J.-D.; Head-Gordon, M. Systematic Optimization of Long-Range Corrected Hybrid Density Functionals. *J. Chem. Phys.* **2008**, *128*, 084106.

(43) Chai, J.-D.; Head-Gordon, M. Long-Range Corrected Hybrid Density Functionals with Damped Atom-Atom Dispersion Corrections. *Phys. Chem. Chem. Phys.* **2008**, *10*, 6615–6620.

(44) Dunning, T. H. Gaussian Basis Sets for Use in Correlated Molecular Calculations. I. The Atoms Boron Through Neon and Hydrogen. *J. Chem. Phys.* **1989**, *90*, 1007–1023.

(45) Narendrapurapu, B. S.; Richardson, N. A.; Copan, A. V.; Estep, M. L.; Yang, Z.; Schaefer, H. F. Investigating the Effects of Basis Set on Metal-Metal and Metal-Ligand Bond Distances in Stable Transition Metal Carbonyls: Performance of Correlation Consistent Basis Sets with 35 Density Functionals. *J. Chem. Theory Comput.* **2013**, *9*, 2930–2938.

(46) Peterson, K. A.; Figgen, D.; Dolg, M.; Stoll, H. Energy-Consistent Relativistic Pseudopotentials and Correlation Consistent Basis Sets for the 4d Elements Y–Pd. *J. Chem. Phys.* **2007**, *126*, 124101.

(47) Figgen, D.; Peterson, K. A.; Dolg, M.; Stoll, H. Energy-consistent Pseudopotentials and Correlation Consistent Basis Sets for the 5d Elements Hf–Pt. *J. Chem. Phys.* **2009**, *130*, 164108.

(48) Neese, F. The ORCA Program System. *WIRES Comput. Mol. Sci.* **2012**, *2*, 73–78.

(49) Wheeler, S. E.; Houk, K. N. Integration Grid Errors for Meta-GGA-Predicted Reaction Energies: Origin of Grid Errors for the M06 Suite of Functionals. *J. Chem. Theory Comput.* **2010**, *6*, 395–404.

(50) Neese, F. An Improvement of the Resolution of the Identity Approximation for the Formation of the Coulomb Matrix. *J. Comput. Chem.* **2003**, *24*, 1740–1747.

(51) Neese, F.; Wennmohs, F.; Hansen, A.; Becker, U. Efficient, Approximate and Parallel Hartree–Fock and Hybrid DFT Calculations. A 'Chain-of-spheres' Algorithm for the Hartree–Fock Exchange. *Chem. Phys.* **2009**, *356*, 98–109.

(52) Tolman, C. A. Electron Donor-Acceptor Properties of Phosphorus Ligands. Substituent Additivity. *J. Am. Chem. Soc.* **1970**, *92*, 2953–2956.

(CO)$_5$Cr=CH$_2$ (CO)$_4$Fe=CH$_2$ (CO)$_3$Ni=CH$_2$